



Research paper

Kynurenine 3-monooxygenase upregulates pluripotent genes through β -catenin and promotes triple-negative breast cancer progression

Tzu-Ting Huang^{a,†}, Ling-Ming Tseng^{a,b,c,†}, Ji-Lin Chen^a, Pei-Yi Chu^{d,e}, Chia-Han Lee^a, Chun-Teng Huang^{b,f}, Wan-Lun Wang^{a,b}, Ka-Yi Lau^a, Mei-Fang Tseng^a, Yuan-Ya Chang^a, Tzu-Yi Chiang^g, Yune-Fang Ueng^{g,h,i}, Hsin-Chen Lee^j, Ming-Shen Dai^k, Chun-Yu Liu^{a,b,l,m,*}

^a Comprehensive Breast Health Center, Taipei Veterans General Hospital, Taipei, Taiwan

^b School of Medicine, National Yang-Ming University, Taipei, Taiwan

^c Division of Experimental Surgery, Department of Surgery, Taipei Veterans General Hospital, Taipei, Taiwan

^d Department of Pathology, Show Chwan Memorial Hospital, Changhua City, Taiwan

^e School of Medicine, Fu Jen Catholic University, New Taipei City, Taiwan

^f Division of Hematology & Oncology, Department of Medicine, Yang-Ming Branch of Taipei City Hospital, Centre, Taipei, Taiwan

^g Institute of Biopharmaceutical Sciences, School of Pharmacy, National Yang-Ming University, Taipei 112, Taiwan

^h Division of Basic Chinese Medicine, National Research Institute of Chinese Medicine, Taipei 112, Taiwan

ⁱ Institute of Medical Sciences, Taipei Medical University, Taipei 101, Taiwan

^j Institute of Pharmacology, School of Medicine, National Yang-Ming University, Taiwan

^k Hematology/Oncology, Tri-Service General Hospital, National Defense Medical, Taiwan

^l Division of Transfusion Medicine, Department of Medicine, Taipei Veterans General Hospital, Taipei, Taiwan

^m Division of Medical Oncology, Center for Immuno-Oncology, Department of Oncology, Taipei Veterans General Hospital, Taipei, Taiwan



ARTICLE INFO

Article History:

Received 15 July 2019

Revised 27 February 2020

Accepted 28 February 2020

Available online xxx

Keywords:

KMO

Triple negative breast cancer

β -catenin

ABSTRACT

Background: Triple-negative breast cancer (TNBC) is aggressive and has a poor prognosis. Kynurenine 3-monooxygenase (KMO), a crucial kynurenine metabolic enzyme, is involved in inflammation, immune response and tumorigenesis. We aimed to study the role of KMO in TNBC.

Methods: KMO alteration and expression data from public databases were analyzed. KMO expression levels in TNBC samples were analyzed using immunohistochemistry. Knockdown of KMO in TNBC cells was achieved by RNAi and CRISPR/Cas9. KMO functions were examined by MTT, colony-forming, transwell migration/invasion, and mammosphere assays. The molecular events were analyzed by cDNA microarrays, Western blot, quantitative real-time PCR and luciferase reporter assays. Tumor growth and metastasis were detected by orthotopic xenograft and tail vein metastasis mouse models, respectively.

Findings: KMO was amplified and associated with worse survival in breast cancer patients. KMO expression levels were higher in TNBC tumors compared to adjacent normal mammary tissues. *In vitro* ectopic KMO expression increased cell growth, colony and mammosphere formation, migration, invasion as well as mesenchymal marker expression levels in TNBC cells. In addition, KMO increased pluripotent gene expression levels and promoter activities *in vitro*. Mechanistically, KMO was associated with β -catenin and prevented β -catenin degradation, thereby enhancing the transcription of pluripotent genes. KMO knockdown suppressed tumor growth and the expression levels of β -catenin, CD44 and Nanog. Furthermore, mutant KMO (known with suppressed enzymatic activity) could still promote TNBC cell migration/invasion. Importantly, mice bearing CRISPR KMO-knockdown TNBC tumors showed decreased lung metastasis and prolonged survival.

Interpretation: KMO regulates pluripotent genes via β -catenin and plays an oncogenic role in TNBC progression.

© 2020 Published by Elsevier B.V. This is an open access article under the CC BY-NC-ND license.

(<http://creativecommons.org/licenses/by-nc-nd/4.0/>)

1. Introduction

Triple-negative breast cancer (TNBC), accounting for 15–20% of breast cancers, lacks hormone receptor expression and human epidermal growth factor receptor 2 (HER2) amplification, is aggressive and has a poor prognostic subtype [1]. TNBC harbors heterogeneous molecular phenotypes, such as BRCA1/2 mutations, presence of

* Corresponding author at: Division of Transfusion Medicine, Department of Medicine, Taipei Veterans General Hospital, No. 201, Sec. 2, Shih-Pai Road, Taipei 112, Taiwan.

E-mail address: cylu3@vghtpe.gov.tw (C.-Y. Liu).

† Tzu-Ting Huang and Ling-Ming Tseng contributed equally to the work.

Research in context

Evidence before this study

Breast cancer exhibits aberrant metabolic profile including triple-negative breast cancer (TNBC). Estrogen receptor negative breast cancer shows high level of tryptophan metabolite kynurenine. Kynurenine 3-monooxygenase (KMO), a key kynurenine pathway enzyme, which contributes to immune tolerance and dysregulation in cancer.

Added value of this study

KMO expressions were higher in TNBC tumors compared to adjacent normal mammary tissues. KMO protein, rather than its enzyme activity, enhanced cell growth, motility and cancer stem cell phenotypes. KMO interacted with β -catenin preventing its degradation. Beta-catenin mediated KMO-induced pluripotent genes expressions. Knockdown of KMO reduced tumor growth and lung metastasis *in vivo*.

Implications of all the available evidence

Our data have disclosed a novel oncoprotein KMO in the regulation of β -catenin which contributes to TNBC progression.

androgen receptor (AR) and PI3K/Akt pathway activation [2]. Currently, single-agent chemotherapy or in combination with surgery or radiotherapy remains the standard treatment for TNBC. No specific therapeutic guidelines have been established [3]. Therefore, developing targeted therapeutic options and defining clinical biomarkers are urgently need for TNBC.

Kynurenine 3-monooxygenase (KMO) is a key kynurenine pathway enzyme localized to the outer membrane of mitochondria [4]. Previous literature suggests that KMO controls the conversion of kynurenine to neuroactive and immunoregulatory tryptophan metabolites [5,6], which contribute to immune tolerance and dysregulation in cancer [7,8]. Recently, KMO has been demonstrated to promote cancer progression and to act as prognostic marker of human hepatocellular carcinoma [9]. KMO also serves as a diagnostic and prognostic biomarker in canine mammary gland tumor [10]. Elevated KMO has been found in all breast invasive carcinoma tissues as well as in normal breast epithelial cells in the immediate tumor proximity [11], implying that KMO expression may influence kynurenine pathway activity in surrounding normal tissue and may be involved in the tumorigenesis of breast cancer. Furthermore, higher levels of tryptophan metabolites, including kynurenine, quin and NAD⁺, were found in patients with TNBC relative to patients with estrogen receptor (ER)-positive breast cancer [12]. Thus far, the roles of KMO have not been demonstrated in TNBC tumorigenesis. Therefore, we aimed to study the biological functions and expression levels of KMO in regard to TNBC progression.

β -catenin is encoded by the CTNNB1 gene and is involved in the regulation of cell-cell adhesion. As a transcription factor, β -catenin mediates canonical Wnt signaling, which controls many biological processes, such as cell fate determination, cell proliferation, and stem cell maintenance [13]. β -catenin degradation is regulated by a protein complex composed of glycogen synthase kinase 3 beta (GSK3 β), adenomatous polyposis coli (APC) and Axin. Once the amino-terminal Thr41, Ser37, and Ser33 residues of β -catenin are phosphorylated, phosphorylated β -catenin is further ubiquitinated by E3 ligases for proteasomal degradation [14,15]. Abnormal regulation of β -catenin degradation leads to various diseases. Increased levels of cytoplasm expression and nuclear localization of β -catenin induce carcinogens and promote cancer cell proliferation and survival [16]. Here, for the

first time, we identified KMO as a novel oncogene in TNBC progression. We observed that KMO promoted cancer aggressiveness by elevating pluripotent genes through β -catenin signaling. Importantly, KMO knockdown suppressed tumorigenesis and led to a prolonged overall survival *in vivo*.

2. Materials and methods

2.1. Patients and specimens

For the use of clinical materials for research purposes, prior patients' consents were obtained and approval was granted from the ethics committee of the Institutional Review Board of Taipei Veterans General Hospital, Taipei City, Taiwan (Protocol No. 2013–10–005A; date of approval: 4 November 2013 and Protocol No. 2017–10–016AC; date of approval: 28 October 2017); the study was conducted in compliance with the Helsinki Declaration. The 96 patients enrolled for this study were informed of the purpose and details regarding the project. The primary TNBC tumor tissues were processed and examined for KMO expression using immunohistochemical staining. All samples were made into a tissue array before staining to optimize the stability of the experimental procedure. The antibody against KMO (LS-C165595, LSBio, Seattle, WA, USA) used in this experiment was obtained from BD Biosciences. KMO expression levels were recorded and interpreted by a certified pathologist. The IHC staining of KMO was assessed semiquantitatively by assigning an H-score (ranging 0–300), which was defined by multiplying the percentage of positive-stained carcinoma cells (from 0–100) by the staining intensity (from negative staining as 0, weak as 1, moderate as 2, to strong staining as 3). A pathologist specializing in breast cancer pathology performed the assessment of the H-scores independently without being given the clinical information on the tumor specimens.

2.2. Cancer genome atlas data description

2.2.1. KMO alterations were downloaded from cbiportal (<http://cbiportal.org/index.do>), and KMO expression data from normal tissues and breast tumor samples were downloaded from The Cancer Genome Atlas (TCGA) (<https://tcga-data.nci.nih.gov/tcga/>). Data processing and quality control were conducted by the Broad GDAC Firehose data portal (<https://gdac.broadinstitute.org/>). The mRNA reads per expectation maximization (RSEM) [17] of all samples were analyzed using GraphPad Prism v 7.1 software.

2.3. Cell culture and reagents

Breast cancer cell lines and MCF10A cells were purchased from American Type Culture Collection (Manassas, VA). All cells were maintained in Dulbecco's Modified Eagle Medium (Gibco) supplemented with 10% FBS, 2-mM L-glutamine, 0.1-mM non-essential amino acids and 1% penicillin/streptomycin in a 5% CO₂ atmosphere at 37 °C. KMO inhibitors, UPF 648 (Axon Medchem, Reston, VA, USA) and Ro 61–8048 (Sigma-Aldrich, St Louis, MO, USA), were dissolved in dimethyl sulfoxide (DMSO). MTT was purchased from Sigma-Aldrich.

2.4. Plasmids, plasmid construction and transfection

The KMO, myc-tagged β -catenin and pCMV6 expression plasmids were purchased from OriGene (Rockville, MD, USA). The KMO mutants expressing KMO^{N363D} and KMO^{Y398F} were cloned using QuikChange Lightning (Agilent, Santa Clara, CA, USA) and verified by sequencing. For transfection, cells were seeded onto 6-cm dish for 24 h and transfected using Lipofectamine 3000 (Thermo Fisher Scientific, Waltham, MA, USA) following to manufacturer's instructions. To knockdown endogenous KMO, MDA-MB-468 and MDA-MB-231 cells were transfected with siRNAs against KMO (L-009897-01) or control

(D-001810-10) (final concentration of 25 μM) using DharmaFECT 1 Transfection Reagent (T-2001-01) according to manufacturer's instructions (Dharmacon, Chicago, IL, USA). Reporter plasmids Nanog-Luc (Nanog), Oct4-Luc (Oct4), or SOX-2-Luc (SOX-2) are gifts from Dr. Muh-Hwa Yang [18]. For reporter assay, the cells were co-transfected with luciferase reporter plasmids and reference renilla luciferase plasmids (pRL-TK) along with either KMO-expressing (XL5-KMO) or pCMV6 plasmids using Lipofectamine 3000 (Thermo Fisher Scientific) for 48 h. The promoter activity was analyzed by dual luciferase assay, according to the manual description (Promega, Madison, WI, USA).

2.5. CRISPR/Cas9 KMO gene editing

A 20-bp KMO single-guide RNA (sgRNA) sequence targeting the first exon of KMO was designed using the online database of predicted protospacer adjacent motif (PAM) targeting site. A two complementary primer set of forward: 5'-CACCGCCCTGACTAAACATTGCCGC-3' and reverse: 5'-AAACGCGGCAATGTTTACTCAGGGC-3' containing *BsmBI* ligation adapters was customized and purchased from Tri-I Biotech (Taipei, Taiwan). The primers (100 μM of each) primer were annealed using a T4 ligase kit following the manufacturer's instructions (New England Biolabs, MA, USA). The product was then purified with a PCR-cleaning Kit (Geneaid, Taipei, Taiwan). The purified KMO sgRNA was ligated into *BsmBI*-digested LentiCRISPR v2 plasmids (Addgene, Watertown, MA, USA) using a Quick Ligation Kit (New England Biolabs, MA, USA). LentiCRISPR constructs (LentiCRISPR v2 or LentiCRISPR v2/KMO sgRNA) were cotransfected with pMD.G and pCMVdeltaR8.91 plasmids into HEK293 cells to generate lentivirus. MDA-MB-231 cells were transduced with lentivirus harboring LentiCRISPR v2 or LentiCRISPR v2/KMO sgRNA and were selected with puromycin. Single colonies were picked and verified by sequencing.

2.6. cDNA microarray and data analysis

The gene expression patterns of control and KMO knockdown cells were analyzed using an Affymetrix Expression HU133 2.0 Microarray. The total RNA collection, complementary RNA probe preparation, array hybridization, feature selection and computational analysis were performed and supported by the High-throughput Genome and Big Data Analysis Core Facility of the National Yang-Ming University VGH Genome Research Center. Data can be found under GEO accession numbers GSE145661. Datasets were quartile-normalized and log-transformed prior to analysis (Supplementary Table 1). The differentially expressed genes (>2-fold change) in MDA-MB-231 cells transfected with siRNA against KMO (siKMO) versus the control (siCon) were analyzed by Ingenuity Pathway Analysis.

2.7. Real-time PCR

Total RNA was extracted using TRIzol reagent (Thermo Fisher Scientific), and cDNA was then synthesized by M-MuLV Reverse Transcriptase (New England BioLabs, Ipswich, MA, USA) with an oligo (dT) 18 primer. For real-time PCR, the cDNA was amplified with primers (Supplementary Table 2) using an ABI StepOne Plus system with Maxima SYBR Green/ROX qPCR Master Mix (Thermo Fisher Scientific) according to the manufacturer's instructions. The relative levels of mRNAs were normalized to GAPDH.

2.8. Western blot analysis

Whole-cell extracts were prepared and analyzed by Western blot as previously reported [19]. Nuclear and cytoplasmic extracts were prepared using Nuclear and Cytoplasmic Extraction reagents (Thermo Fisher Scientific) according to the manufacturer's instructions. The cell fraction extracts were validated and quantified by

Western blotting for markers that specifically expressed in each of fractions. The antibodies against KMO (Abcam, Cambridge, MA, United Kingdom), Nanog, CD44, SOX2, E-cadherin, N-cadherin, Twist, Lamin B and β -actin (Cell Signaling, Danvers, MA, USA), and Ub (Santa Cruz Biotechnology, Dallas, Texas, USA) were used.

2.9. Coimmunoprecipitation (CoIP)

The whole-cell extracts were lysed in IP lysis buffer with a Halt Protease and Phosphatase Inhibitor Cocktail (Thermo Fisher Scientific). Protein G sepharose (GE Healthcare Life Sciences, Marlborough, MA, USA) was washed with IP lysis buffer to obtain a 50% (v/v) slurry. Primary antibody (5 μl) and a 50- μl slurry of Protein G sepharose were added into 450 μl of IP lysis buffer and rotated at 4 $^{\circ}\text{C}$ for 2 h to prepare an antibody-bead mixture. Immunoprecipitation was performed by mixing whole-cell extracts and antibody-conjugated protein G sepharose at 4 $^{\circ}\text{C}$ for 4 h. A 30 μl volume of 2 \times Laemmli Sample Buffer was added to the pelleted beads and boiled at 95 $^{\circ}\text{C}$ for 5 min and then analyzed by sodium dodecyl sulfate-polyacrylamide gel electrophoresis.

2.10. Chromatin immunoprecipitation assay

Briefly, MDA-MB-468 cells were transfected with KMO expression or pCMV6 plasmids. After 48 h, cells were harvested and washed with PBS and then fixed with 1% paraformaldehyde at room temperature for 10 min. Nuclear extracts were prepared by nuclear and cytoplasmic extraction reagents with Halt Protease and Phosphatase Inhibitor Cocktail (Thermo Fisher Scientific). Anti- β -catenin or anti-IgG antibodies (5 μl) and 50 μl of a 50% (v/v) slurry of protein G sepharose were added into 450 μl of IP buffer and then rotated at 4 $^{\circ}\text{C}$ for 1 h to prepare the slurry of antibody-conjugated protein G sepharose. Immunoprecipitation was assayed by mixing antibody-conjugated protein G sepharose and nuclear extracts. The mixture was rotated and incubated at 4 $^{\circ}\text{C}$ for 4 h. The DNA was eluted and purified for real-time PCR analysis. The primers used to amplify DNA fragments of Nanog, OCT4 and SOX2 promoters were listed in Supplementary Table 2.

2.11. Colony and mammosphere formation assays

For colony formation assay, the transfected cells were seeded for the assay of anchorage-independent growth in soft agar. Two weeks later, the colonies larger than 0.1 mm in diameter were counted from 10 random fields under the microscope. For mammosphere formation assay, a total of 300 treated cells were suspended in stem cell-selective conditions and then seeded onto 96-well ultra-low attachment plates. 11 days later, the spheres larger than 50 μm in diameter were counted under the microscope.

2.12. Migration and invasion assays

As described previously [20], the migration and invasion assays were conducted in 24-well plate for 20 h. The treated cells (3×10^4) in 200 μl of serum free medium were seeded onto upper Cell Culture Insert with 8 μm pores (Greiner Bio One, Kremsmünster, Austria) and Matrigel matrix (Corning, New York, NY, USA) coated Cell Culture Insert for migration and invasion assays respectively. The lower chamber was added 900 μl of culture medium. Cells were fixed with methanol for 10 min and stained with 0.05% crystal violet for 1 h. The migrated or invaded cells were counted under the microscope from 10 random fields.

2.13. GSK3 β assay

To measure GSK3 β activity, a Kinase-Glo-based assay was used (BPS Bioscience, San Diego, CA, USA). A 25- μ l master mix containing 5 μ l of 5 \times kinase assay buffer, 1 μ l of ATP (500 μ M), 5 μ l of GSK substrate peptide (1 mg/ml) and 14 μ l of distilled water was prepared. Twenty-five microliters of master mixture and 25 μ l of cell lysates were added into each well and incubated at 30 $^{\circ}$ C for 45 min. Kinase-Glo Max reagent (50 μ l, Promega) was added into each well and further incubated at room temperature for 15 min, protected from light. The luminescence was determined by microplate reader.

2.14. Determination of L-kynurenine and 3-hydroxykynurenine

The concentrations of L-kynurenine and 3-hydroxykynurenine (3-HK) in cultured medium were measured using liquid chromatography-mass spectrometry (LC-MS) following the method reported by Fuertig et al. [21]. For standard preparation, kynurenine (Sigma-Aldrich) and 3-HK (Toronto Research Chemicals, Ontario, Canada) were dissolved in deionized water, and a 1/9 vol of 60% HClO₄ was then added. Fifteen microliters of culture medium were added to 15 μ l of acidified mobile phase (0.2% formic acid/0.05% trifluoroacetic acid/1% acetonitrile in water). Then, 150 μ l of ice-cold 100% methanol was added, and the mixture was incubated at -20 $^{\circ}$ C for 30 min. The mixture was centrifuged at 3000 \times g for 15 min at 4 $^{\circ}$ C. The supernatant was dried under a gentle stream of nitrogen and reconstituted in 50 μ l of acidified mobile phase. A 20 μ l sample was injected into an LC-MS system (LCMS-2020, Shimadzu Co., Kyoto, Japan). Separation was performed using a C18 column (2.6 μ m, 2.1 mm \times 100 mm, Fortis Technol. Ltd. UK) and a mobile phase constituted of a stepwise gradient of A (0.1% formic acid in water) and mobile phase B (0.2% formic acid) at a rate of 0.4 ml/min. The gradient for LC-MS is listed in Supplementary Table 3. The sample was detected using absorbance at 220 nm by a PDA detector. The specific mass-to-charge ratios (*m/z*) are listed in Supplementary Table 4.

2.15. Measurement of KMO activity

A KMO inhibitor screening assay kit was purchased from BPS Bioscience (San Diego, CA, USA). To determine the efficacy of KMO inhibitor, 50 μ l of KMO protein (20 mg/ml), 10 μ l of inhibitor and 40 μ l of KMO substrate mixture (0.44 μ M NADPH and 0.88 μ M L-kynurenine) were added into a 96-well UV-transparent microplate. To determine KMO activity in cell lysates, 5- μ l aliquots of whole-cell extracts, 55 μ l of KMO assay buffer and 40 μ l of KMO substrate mixture were added into the microplate. The UV absorption at 340 nm was measured. The plate was further incubated at room temperature for 90 min. The amount of NADPH remaining in the reaction was measured at 340 nm by a microplate reader. The time 0 measurement was subtracted from the final timepoint at 90 min to account for NADPH absorbance.

2.16. Determination of quinolinic acid concentration

The quinolinic acid (QA) level was determined by an ELISA kit (Cloud-Clone Corp., Katy, TX, USA). Briefly, cell culture supernatants were collected and centrifuged at 1000 \times g for 20 min. A 50- μ l sample was added into each well, and 50 μ l of detection reagent A was then added immediately. The plate was covered with a plate sealer and incubated at 37 $^{\circ}$ C for 1 h. The solution was removed and washed with 350 μ l of wash solution 3 times. One hundred microliters of detection reagent B was added into each well, and the plate was then incubated at 37 $^{\circ}$ C for 30 min and washed 5 times with wash solution. Ninety microliters of substrate solution was added into each well, and the plate was then incubated 37 $^{\circ}$ C for 20 min, protected from light, after which 50 μ l of stop solution was added. The concentration

of QA was measured at 450 nm by a microplate reader. Data were analyzed by CurveExpert 1.4 software.

2.17. Xenograft tumor growth

All animal experiment was conducted under an approved by Institutional Animal Care and Use Committee of Taipei Veterans General Hospital (IACUC No. 2017-258). Female BALB/c nu/nu mice (5-7 weeks of age) were purchased from the National Laboratory Animal Center (Taipei, Taiwan) and maintained in an SPF-environment. Each mouse was subcutaneously injected in the dorsal flank with 5 \times 10⁶ control cells or KMO-knockdown cells suspended in 100 μ l of a 1:1 mixture of phosphate-buffered saline (PBS) and Matrigel (BD Biosciences, Bedford, MA, USA). The volume of tumor was measured three times per week using the standard formula width² \times length \times 0.52. All mice were sacrificed on day 70, and the xenografted tumors were harvested and assayed for subsequent experiments.

2.18. Immunohistochemical staining

Immunohistochemical staining procedure has been described [22]. Briefly, primary antibodies against KMO (LS-C165595, LSBio, Seattle, WA, USA), CD44 (#3570), β -catenin (#8480S) and Nanog (#4903; Cell Signaling) were used at 1:100 dilution for overnight incubation. The slides were then counterstained with hematoxylin stain solution. Rabbit IgG was used as a control for antibody specificity. Staining signals were detected using the EnVision™ system (Dako, Santa Clara, CA, USA).

2.19. Tail vein metastasis assay

NOD-SCID immunodeficient female mice aged 5 weeks were purchased from the National Laboratory Animal Center (Taipei, Taiwan) and maintained in an SPF-environment. CRISPR KMO-knockdown or control cells were seeded 1 \times 10⁶ cells responded in 100 μ l of PBS and intravenously injected into the tail veins. Animals were sacrificed on Day 61 after injection, the metastatic nodules on the lungs surface were counted and quantified.

2.20. Statistical analysis

Data are expressed as mean \pm SD or mean \pm SEM. Statistical comparisons were based on nonparametric tests, and statistical significance was defined as a *P* value less than 0.05. Quantification of protein levels was analyzed by ImageJ software. For survival analysis, survival curves of mice were generated by the Kaplan-Meier method and compared by Log-rank test. All statistical analyses were performed using GraphPad Prism v. 7.1 (GraphPad Software).

3. Results

3.1. KMO amplification in patients with breast cancer and TNBC

We first analyzed the gene alteration frequencies of KMO, kynureninase (KYNU) and kynurenine aminotransferase (KAT) isoenzymes, which have been reported to metabolize kynurenine [7]. Among others, KMO was the most frequently altered gene found in ~5–30% of breast tumors in eight breast cancer databases (Fig. 1a). We further analyzed KMO expression data from The Cancer Genome Atlas (TCGA) in breast cancer and TNBC specimens compared to normal tissues. KMO transcripts were increased in patients with breast cancer and TNBC (Fig. 1b, c). We also collected and examined the samples from patients with TNBC and found that KMO was upregulated in TNBC tissues (Fig. 1d, left). The protein levels of KMO were also elevated in tumor tissues relative to paired mammary epithelial samples by immunohistochemical analysis (Fig. 1d, right). In fact, the results

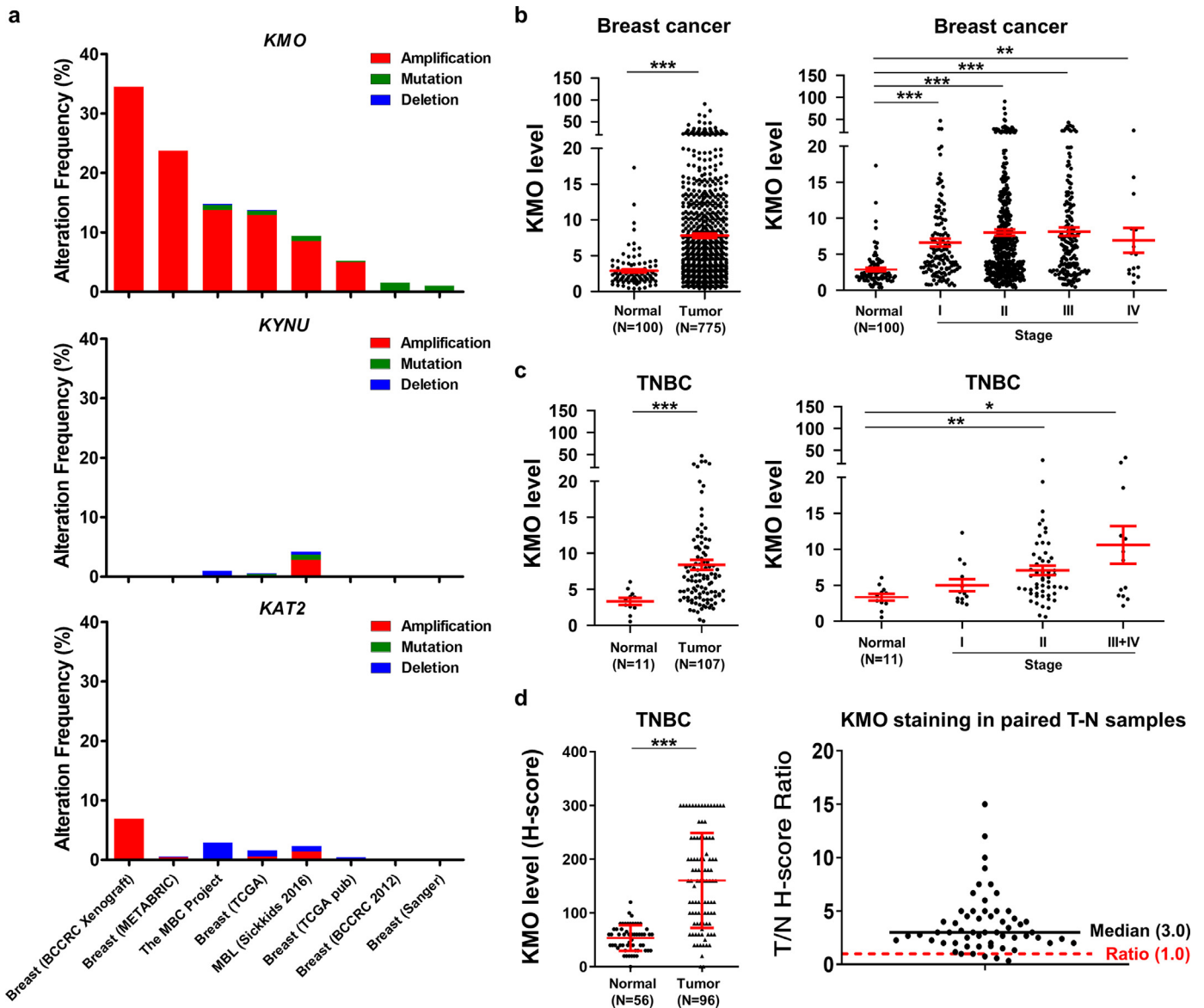


Fig. 1. Up-regulation of KMO in patients with TNBC. (a) The gene alteration frequencies of *KMO*, *KYNU* and *KAT2* in breast cancer databases. (b, c) The level 3 data of *KMO* mRNA RPKM (Reads Per Kilobase per Million mapped reads) from patients with breast cancer (b) and TNBC (c) were selected and analyzed from the TCGA database. (d) The IHC intensity of *KMO* was determined independently by a qualified pathologist, and a H-score of 0–300 based on percentage of cells stained at different intensities were assigned to each in-house TNBC samples (left). The ratio of tumor to normal *KMO* IHC H-score was illustrated (right). Data are shown as mean \pm SD. Student's *t*-test, *, $P < 0.05$; **, $P < 0.01$; ***, $P < 0.001$.

showed that *KMO* levels in tissues from all breast cancer subtypes were higher than in normal tissues (Figure S1a, b). To evaluate the clinical relevance of *KMO* in breast cancer, data from public cancer datasets, Kaplan-Meier-plotter [23], Gene Expression Omnibus (<https://www.ncbi.nlm.nih.gov/geo/>) and UCSC Xena (<http://xena.ucsc.edu>) were examined. A high level of *KMO* was associated with worse recurrence-free survival (RFS; Figure S1c) and distant metastasis-free survival (DMFS; Figure S1d). Additionally, we conducted analysis using the biomarker validation database SurvExpress [24], and found that high risks of metastasis and recurrence were linked to high *KMO* expression levels (Figure S1e). These data suggested that *KMO* was upregulated in patients with breast cancer and might participate in metastasis and recurrence.

3.2. *KMO* acts as an oncogene in TNBC cells

We next analyzed the endogenous levels of *KMO* in a panel of breast cancer cell lines, and the results showed that *KMO* protein

expression levels were high in breast cancer cell lines, including TNBC, in comparison with breast epithelial MCF10A cells (Fig. 2a). To address the biological functions of *KMO* in TNBC, the *KMO*-expression or control plasmids were transiently transfected into TNBC cells. Exogenous *KMO* increased the cell growth and colony-forming capacity of MDA-MB-231 and MDA-MB-468 cells. In contrast, knockdown of *KMO* suppressed cell growth and colony formation (Fig. 2b, c). Since *KMO* is located on the outer membrane of mitochondria [4], we checked whether *KMO* inhibition affected mitochondrial functions. However, knockdown of *KMO* did not affect the mitochondrial functions, including oxygen consumption rate (OCR; Figure S2a) and the basal extracellular acidification rate (ECAR; Figure S2b). We observed that *KMO* knockdown MDA-MB-231 cells showed rounded morphology, while *KMO*-expressing MDA-MB-468 cells showed spindle-like morphology (Fig. 2d). To further investigate whether *KMO* regulated cell motility, transwell migration and invasion assays were performed. Ectopic *KMO* expression promoted cell migration and invasion. Moreover, cell motility was reduced by *KMO*

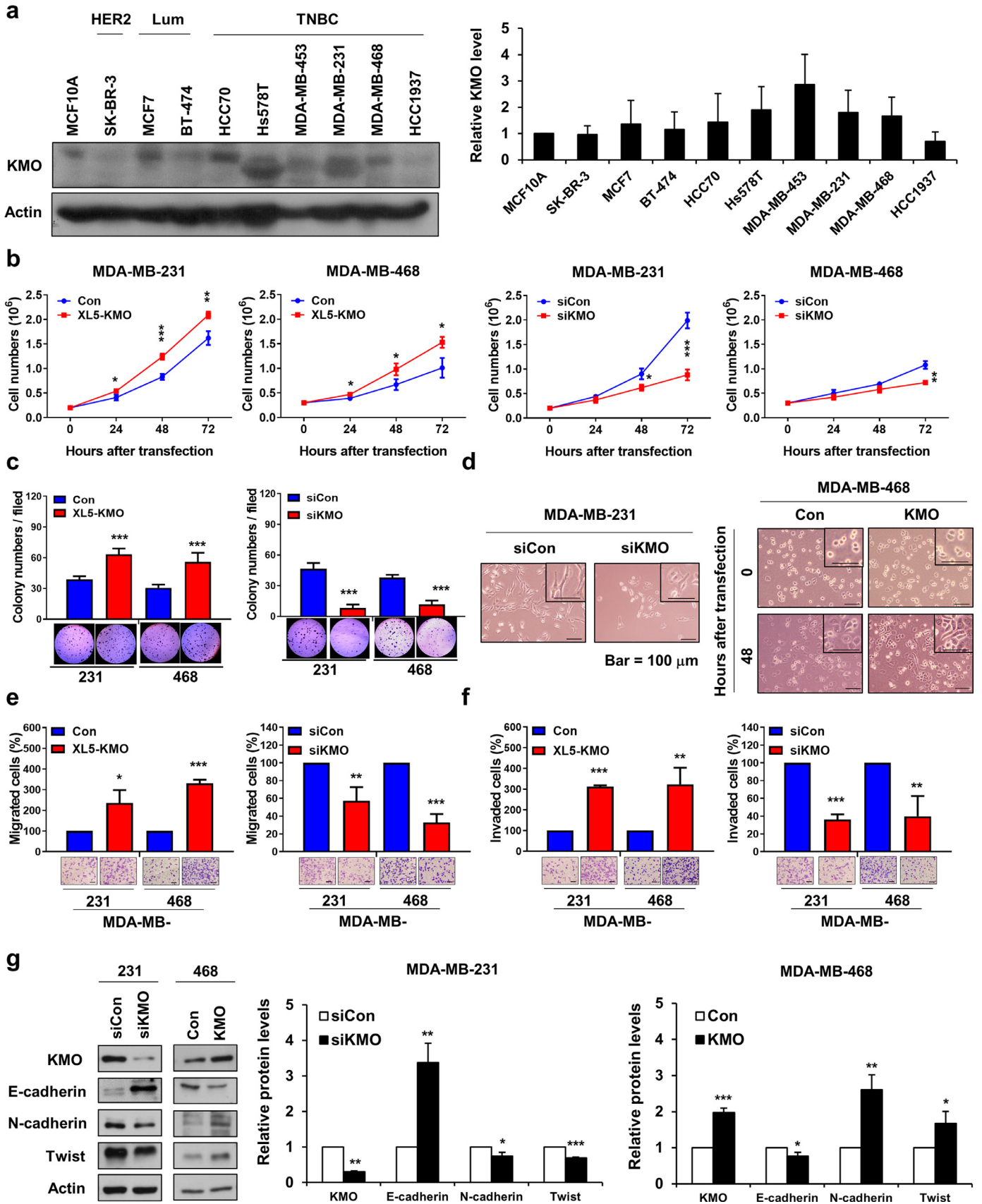


Fig. 2. KMO enhances TNBC progression in vitro. (a) The protein levels of KMO in MCF10A and breast cancer cell lines were determined by Western blot (left). The results were quantified (right). (b–g) MDA-MB-231 and MDA-MB-468 cells were transfected with KMO-expressing (XL5-KMO) or pCMV6 control plasmids (Con) and siRNA against KMO (siKMO) or control (siCon) for 48 h. The transfected cells were assessed by trypan blue exclusion assay (b), colony assay (c), morphology observation (d), migration assay (e), invasion assay (f) and Western blot analysis (g, left). The blottings were quantified (g, right). Data are representative of three independent experiments. Columns, mean ($N = 3$); bars, SD. Student's *t*-test, *, $P < 0.05$; **, $P < 0.01$; ***, $P < 0.001$.

knockdown (Fig. 2e, f). In addition to morphology change and motility elevation, the epithelial-mesenchymal transition (EMT) phenotype can be examined by the loss of epithelial markers and the acquisition of mesenchymal markers. Consistently, knockdown of KMO increased the level of the epithelial marker E-cadherin and decreased the levels of mesenchymal markers, including N-cadherin and Twist, whereas these effects were reversed by KMO overexpression (Fig. 2g).

3.3. KMO enhances the stemness property of TNBC cells

To investigate the regulatory mechanisms of KMO-mediated TNBC progression, we then identified KMO target genes by conducting a cDNA microarray of MDA-MB-231 cells transfected with siRNA against KMO or control. We identified a group of KMO-regulated genes that are involved in cellular movement, cell death and survival, cellular development, cellular growth and proliferation, as well as cell-to-cell signaling and interaction (Fig. 3a). In addition, KMO silencing not only decreased the pluripotent gene expression levels of *CD44*, *Nanog*, *POU5F1* (OCT4) and *SOX2* but also suppressed the expression of *CTNBN1* (β -catenin) (Fig. 3b), which is a well-known upstream regulator of pluripotent genes and the cancer stem cell (CSC) phenotype [25,26]. The existence of CSCs plays a role in metastasis formation [27]. Moreover, previous research has shown that EMT can induce differentiated cancer cells into a CSC-like phenotype [28]. KMO-expressing cells exhibited mesenchymal-like phenotypes (Fig. 2d-g). Thereby, we hypothesized that KMO might be involved in the regulation of TNBC CSCs. To test our hypothesis, we first confirmed the expression levels of stemness markers by real-time PCR. Consistent with the cDNA microarray results, we observed decreases in the mRNA expression levels of *CD44*, *Nanog*, *OCT4* and *SOX2* in KMO-knockdown MDA-MB-231 cells, whereas the expression levels were increased in KMO-expressing MDA-MB-468 cells (Fig. 3c). The protein expression levels of *Nanog*, *SOX2* and *OCT4* were decreased by KMO knockdown, whereas the expression levels were increased by KMO overexpression (Fig. 3d). We then evaluated whether KMO regulated the formation of CSCs by mammosphere assay. Data revealed that KMO suppression decreased the number of mammospheres, while exogenous KMO increased the mammosphere-forming capacity (Fig. 3e). To further analyze whether KMO modulated the transcription of stemness markers, a luciferase reporter assay was conducted. The promoter activities of *Nanog*, *OCT4* and *SOX2* were driven by KMO overexpression (Fig. 3f). Collectively, the results suggested that KMO improved the mammosphere-forming capacity and upregulated the expression levels of pluripotent genes in TNBC cells.

3.4. KMO regulates pluripotent genes through β -catenin

KMO is a hydroxylase enzyme without a putative DNA-binding element; however, we found that KMO regulated *CD44*, *Nanog*, *OCT4* and *SOX2* expression levels and that of their common upstream regulator, β -catenin (Fig. 3). We thus proposed that KMO might regulate these pluripotent genes through β -catenin signaling. To decipher the regulatory mechanism, we next explored the role of β -catenin in KMO-induced pluripotent gene expression. We established KMO-knockdown MDA-MB-231 cell lines using the CRISPR/Cas9 system (CRISPR KMO-KD). The protein expression levels of β -catenin and *CD44* as well as mammosphere numbers were lower in CRISPR KMO-KD cells relative to control cells (Fig. 4a, b and S3a). In addition, *CD44* and β -catenin mRNA expression levels were suppressed in CRISPR KMO-KD cells (Fig. 4c). We found that KMO was expressed in both the cytoplasm and nucleus (Fig. 4d). Importantly, not only cytosolic but also nuclear β -catenin expression was decreased in CRISPR KMO-KD cells compared to parental cells (Fig. 4e). Interestingly, CRISPR KMO-KD increased the level of phosphorylated β -catenin (p- β -catenin), which was further enhanced by treatment with the proteasome inhibitor

carfilzomib (Fig. 4f and S3b). Knockdown of KMO by siRNA-induced p- β -catenin was enhanced by carfilzomib in MDA-MB-468 cells (Fig. 4g and S3c). Additionally, overexpression of KMO decreased β -catenin phosphorylation (Figure S3d). To study whether KMO upregulated β -catenin expression through stabilization, we performed a cycloheximide (CHX) chase assay. The results indicated that ectopic expression of KMO attenuated β -catenin degradation (Fig. 4h and Figure S3e). KMO-expressing cells showed lower ubiquitin levels compared to control cells (Figure S3f). To test whether KMO interacted with β -catenin, the association between KMO and β -catenin was examined by coimmunoprecipitation. β -catenin was immunoprecipitated by antibodies against β -catenin and KMO but not IgG (Fig. 4i and S3g). GSK3 β phosphorylates β -catenin and is essential for β -catenin stabilization. We also found that KMO was immunoprecipitated by antibodies against GSK3 β (Fig. 4j and S3h). Furthermore, the association between β -catenin and GSK3 β was attenuated in KMO-expressing cells compared to control cells (Figure S3i). We found an approximate 25% reduction of GSK3 β activity in KMO-expressing cells (Figure S3j). Next, we aimed to validate whether KMO-regulated pluripotent gene expression levels through β -catenin. The binding of β -catenin to *Nanog*, *OCT4* and *SOX2* promoters was enhanced by KMO overexpression (Fig. 4k). The decreased expression levels of *CD44*, *OCT4* and *SOX2* in KMO-knockdown cells were restored by β -catenin overexpression (Fig. 4l and S3k). These findings demonstrated that KMO was involved in the regulation of β -catenin stability and modulated pluripotent genes via β -catenin.

3.5. KMO promotes TNBC progression irrelevant to its enzyme activity

To study whether KMO-fostered TNBC tumorigenesis was dependent on its enzyme activity, we used two different KMO inhibitors, UPF 648 and Ro 61–8048 [29]. KMO catalyzes the NADPH-dependent hydroxylation. To measure KMO enzymatic inhibition, we determined the consumption of NADPH. The KMO activity was significantly impaired by UPF 648 and Ro 61–8048 (Fig. 5a). Moreover, the level of quinolinic acid (QA), a metabolite of the KMO pathway, was reduced by UPF 648 and Ro 61–8048 treatment (Figure S4a). Surprisingly, inhibition of KMO activity did not affect either the cell viability or migration capacity of TNBC cells (Fig. 5b, c). KMO inhibitors did not alter the protein expression levels of KMO and β -catenin (Fig. 5d). To evaluate whether exogenous KMO was enzymatically active, we measured the levels of L-kynurenine and 3-HK. The results of LC-MS showed increased 3-HK levels in KMO-expressing cells compared to control cells (Fig. 5e). In addition, KMO activity was higher in KMO-expressing cells than in control cells (Figure S4b). The residues N363 and Y398 are known to be essential for KMO enzyme activity, whereas mutations at N363 and Y398 significantly decreased KMO activity [30]. To further investigate the role of functional inactivation of KMO in TNBC progression, we cloned KMO^{N363D} and KMO^{Y398F} expression constructs. Both the protein and mRNA expression levels of β -catenin were upregulated by KMO and mutants (Fig. 5f, g and S4c). Overexpression of wild-type KMO elevated QA levels compared to control cells. In contrast, QA levels were reduced by overexpression of KMO mutants (Fig. 5h). In particular, the cell viability and migration capacity were promoted by KMO^{N363D} and KMO^{Y398F} overexpression (Fig. 5i, j). These findings suggested that the tumor-promoting effects of KMO were independent of enzyme activity.

3.6. KMO promotes TNBC progression and metastasis in vivo

To explore the role of KMO in tumorigenesis *in vivo*, nude mice were subcutaneously implanted with KMO-knockdown or control MDA-MB-231 cells. The results showed that knockdown of KMO reduced tumor growth and slightly decreased tumor weight (Fig. 6a, b). The decreased levels of KMO, β -catenin, *CD44*, and *Nanog* in KMO-knockdown xenografts were confirmed by Western blot and IHC (Fig. 6c, d). To evaluate the effect of KMO elimination on the

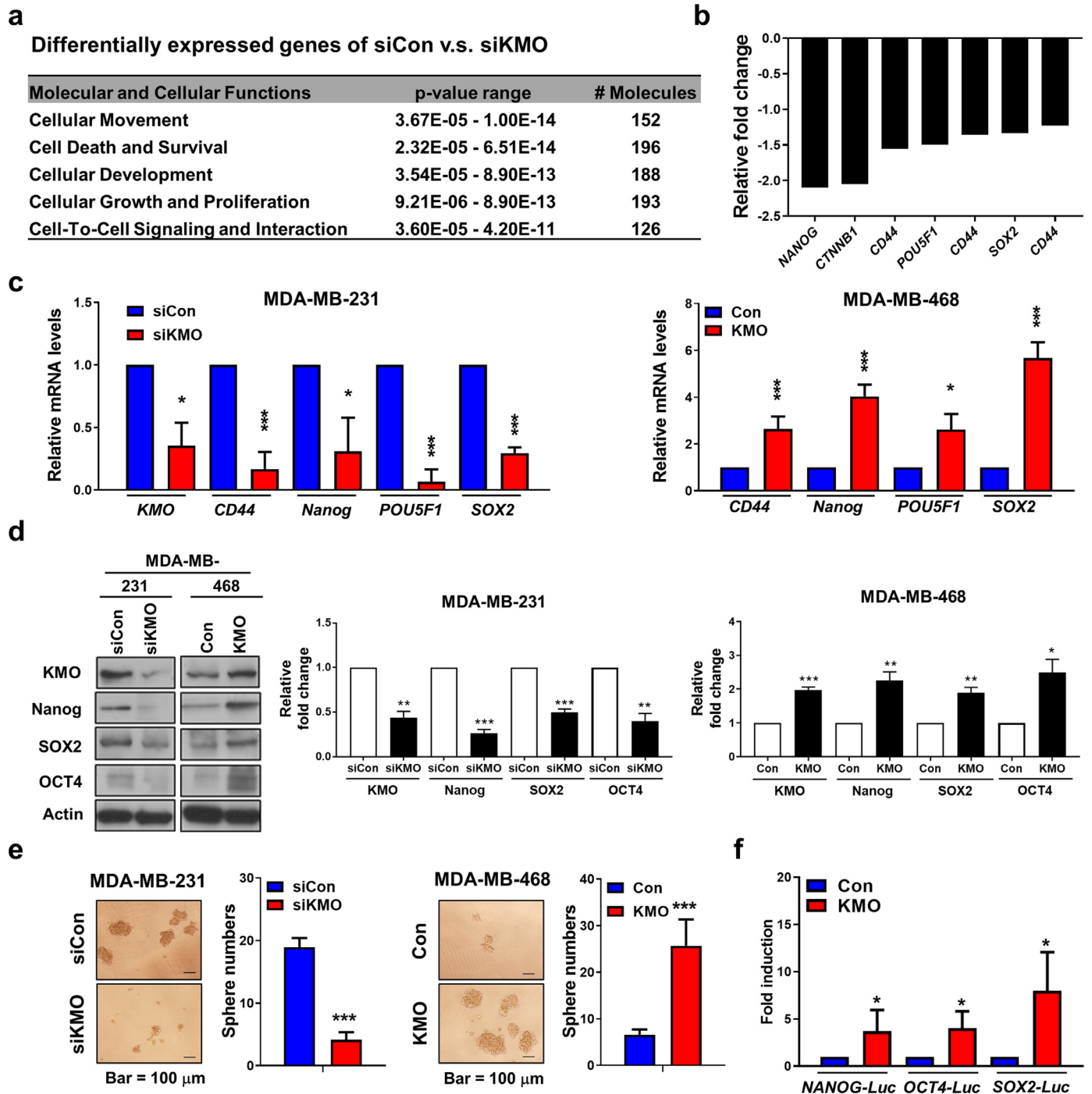


Fig. 3. KMO promotes stemness property of TNBC cells. (a) The differentially expressed genes (>2-fold change) in MDA-MB-231 cells transfected with siRNA against KMO (siKMO) or the control (siCon) were analyzed by Ingenuity Pathway Analysis. The top five molecular and cellular functions are shown. (b) The cDNA microarray data showed the pluripotent gene expressions of *CD44*, *Nanog*, *POU5F1* (*OCT4*), *SOX2*, and *CTNNB1* (β -catenin) were downregulated in KMO knockdown MDA-MB-231 cells compared to control cells. (c-e) MDA-MB-231 cells were transfected with siRNAs against KMO (siKMO) or control (siCon) for 48 h. MDA-MB-468 cells were transfected with KMO-expressing (XL5-KMO) or pCMV6 control plasmids (Con) for 48 h. The transfected cells were assessed by real-time PCR analysis (c), Western blot analysis (d, left), the quantitative results of Western blottings (d, right) and mammosphere assay (e). (f) Reporter plasmids containing *Nanog*, *OCT4* and *SOX2* promoter were co-transfected with KMO-expressing or control plasmids for reporter gene assay. Columns, mean ($N = 4$); bars, SD. Student's *t*-test, *, $P < 0.05$; **, $P < 0.01$; ***, $P < 0.001$.

metastatic colonization of TNBC cells, CRISPR KMO-KD cells were intravenously injected into the tail veins of NOD-SCID immunodeficient mice. The results showed that the lung metastasis capacity was significantly inhibited by CRISPR KMO-KD (Fig. 6e, f). Moreover, in the control group, 5 mice were dead after inoculation within 7 weeks, and only 2 mice survived until the end of the experiment (2/7). In contrast, all mice transplanted with CRISPR KMO-KD cells survived until the end of the experiment (8/8), suggesting that KMO

silencing led to an increased overall survival compared to the control group (Fig. 6g). Taken together, the results indicated that KMO enhanced tumor growth and metastasis of TNBC *in vivo*.

4. Discussion

Breast cancer is still the major cause of cancer death in women worldwide. In addition to common surgery and radiation, there are

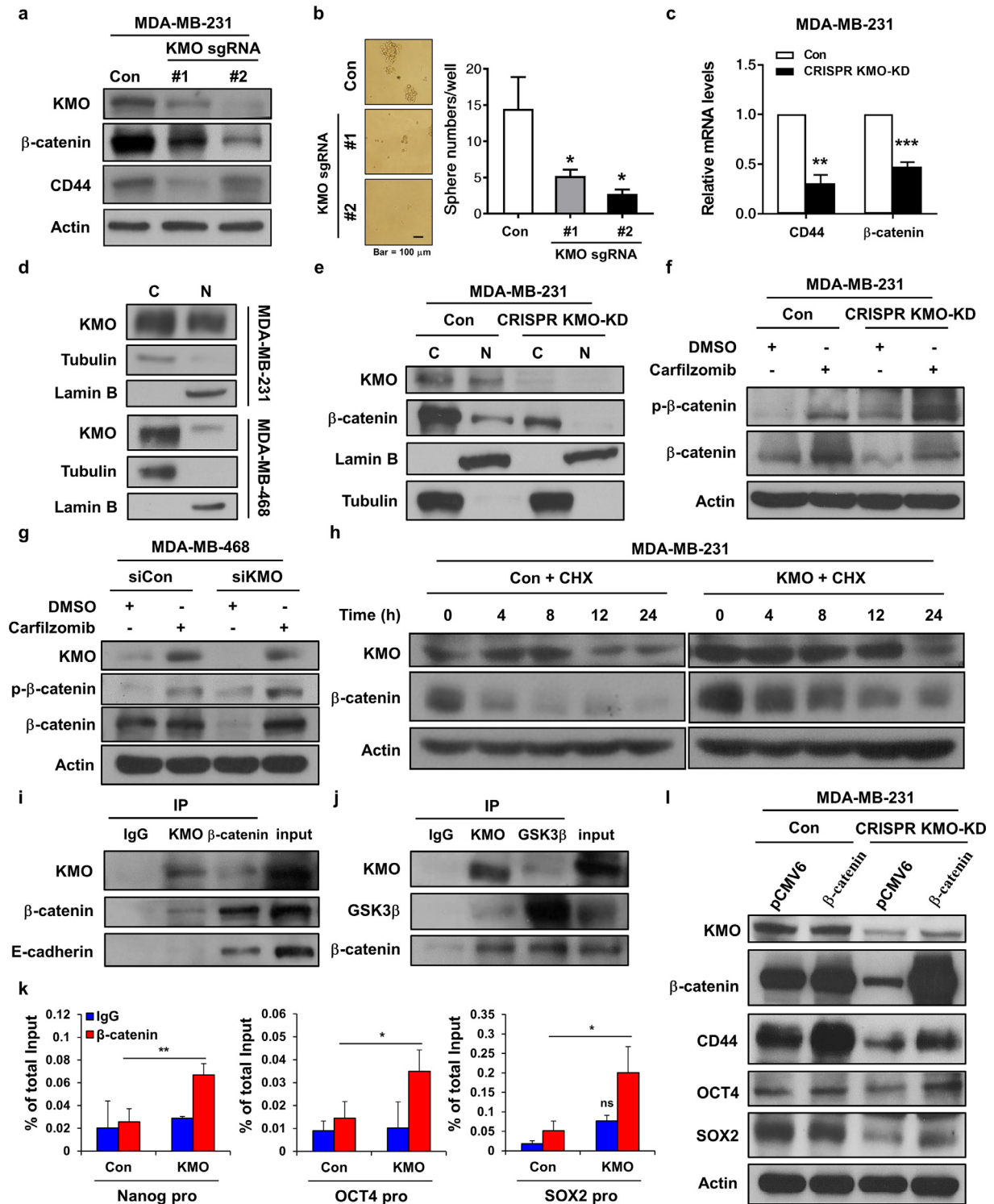


Fig. 4. β -catenin mediates KMO-regulated pluripotent genes. (a) Whole-cell extracts of two CRISPR KMO-KD cell lines and MDA-MB-231 control cells were examined by Western blot analysis. (b) Two CRISPR KMO-KD and parental MDA-MB-231 cell lines were assessed by mammosphere assay. (c) The mRNA levels of β -catenin and CD44 in control and CRISPR KMO-KD cells were determined by real-time PCR. (d) The cytoplasmic and nuclear fractions of MDA-MB-231 and MDA-MB-468 cells were analyzed by Western blotting. (e) The cytoplasmic and nuclear fractions of CRISPR KMO-KD and control cells were analyzed by Western blotting. (f) CRISPR KMO-KD and control cells treated with 50 nM carfilzomib for 20 h were analyzed by Western blot analysis. (g) MDA-MB-468 cells transfected with siRNA against KMO (siKMO) or control (siCon) for 48 h were treated with 50 nM carfilzomib for 20 h. Whole-cell extracts were examined by Western blot analysis. (h) MDA-MB-231 cells transfected with KMO-expressing or control (pCMV6) plasmids for 48 h were further treated with cycloheximide (CHX) for indicated times. Whole-cell extracts of treated cells were analyzed by Western blotting. (i) Whole-cell extracts of MDA-MB-231 cells were harvested for CoIP using antibodies against IgG, KMO or β -catenin. The precipitated proteins were analyzed by Western blot analysis using anti-KMO, anti- β -catenin and anti-E-cadherin (as positive control) antibodies. (j) Whole-cell extracts were harvested for CoIP assay using antibodies against IgG, KMO and GSK3 β . The precipitated proteins were analyzed by Western blot analysis using anti-KMO, anti- β -catenin and anti-GSK3 β antibodies. (k) MDA-MB-468 cells transfected with KMO-expressing or pCMV6 (Con) plasmids were harvested for chromatin immunoprecipitation assay using anti-IgG and anti- β -catenin antibodies. The immunoprecipitated DNAs were amplified the PCR products of Nanog, OCT4 and SOX2 promoters. Percentages of the immunoprecipitated DNAs were examined by real-time PCR and normalized to total input DNA. (l) CRISPR KMO-KD and control cells transfected with β -catenin-expressing construct or pCMV6 vector for 48 h were examined by Western blot analysis. Data are representative of three independent experiments. Columns, mean ($N = 3$); bars, SD. Student's t -test, *, $P < 0.05$; **, $P < 0.01$; ***, $P < 0.001$.

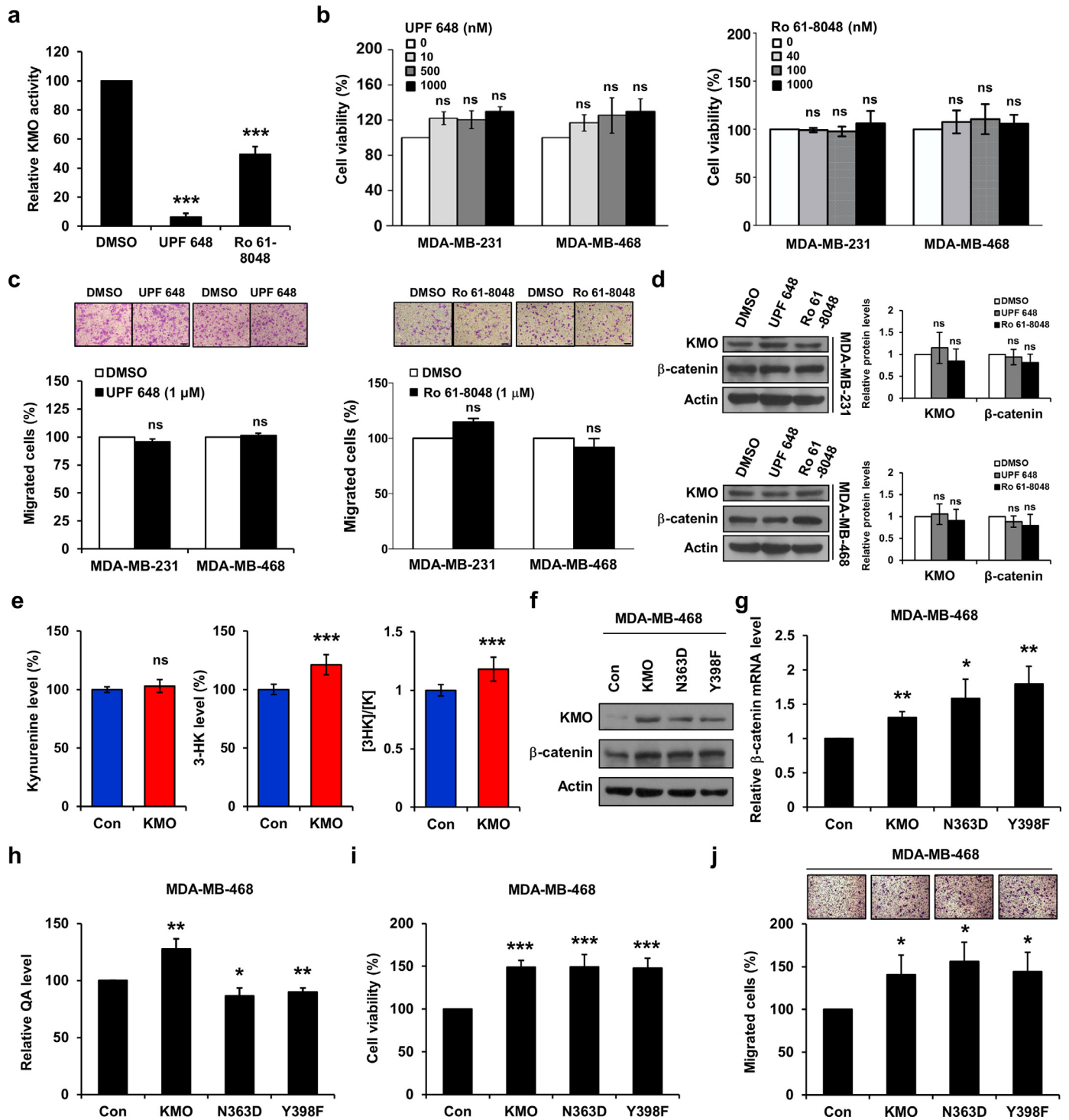


Fig. 5. KMO promotes cell viability and migration irrelevant to its enzyme activity. (a) The efficacies of UPF 648 (1 μM) and Ro 61-8048 (1 μM) were examined by the KMO inhibitor assay. The KMO activity was determined by NADPH absorbance. (b-d) MDA-MB-231 and MDA-MB-468 cells treated with indicated dose of UPF 648 and Ro 61-8048 were examined by MTT assay (b), migration assay (c), Western blot analysis using antibodies against anti-KMO, anti-β-catenin and anti-Actin (d, left) and the quantitative results of Western blotting (d, right). (e) The levels of L-kynurenine and 3-HK were examined by LC-MS. (f-j) MDA-MB-468 cells transfected with KMO, KMO mutants (N363D and Y398F) expression constructs or pCMV6 plasmids (Con) were analyzed by Western blot analysis using antibodies against KMO, β-catenin and Actin (f), real-time PCR (g), the QA ELISA analysis (h), MTT (i) and migration assay (j). Columns, mean (N = 3); bars, SD. Student's *t*-test, *, *P* < 0.05; **, *P* < 0.01; ***, *P* < 0.001.

many types of drugs that target hormone receptors or growth factor inhibitors. However, TNBC is known for the absence of hormone receptors and HER2, thus resulting in a more aggressive behavior and increased treatment difficulty [31]. Tryptophan metabolism is important for tumorigenesis. Tang X. et al. discovered that tumor metabolism was different between ER-positive and ER-negative breast cancer. ER-negative breast cancer showed high levels of the

tryptophan metabolite, kynurenine, which has been linked to IDO expression [32]. Consistently, the expression levels of serum kynurenine and IDO1 mRNA were higher in patients with ER-negative breast cancer than in those with ER-positive breast cancer [33]. In addition, suppression of IDO1 expression by hypermethylation of the IDO1 promoter is more characteristic of ER-positive than ER-negative breast cancer [33,34]. Previous studies also suggest that TNBC

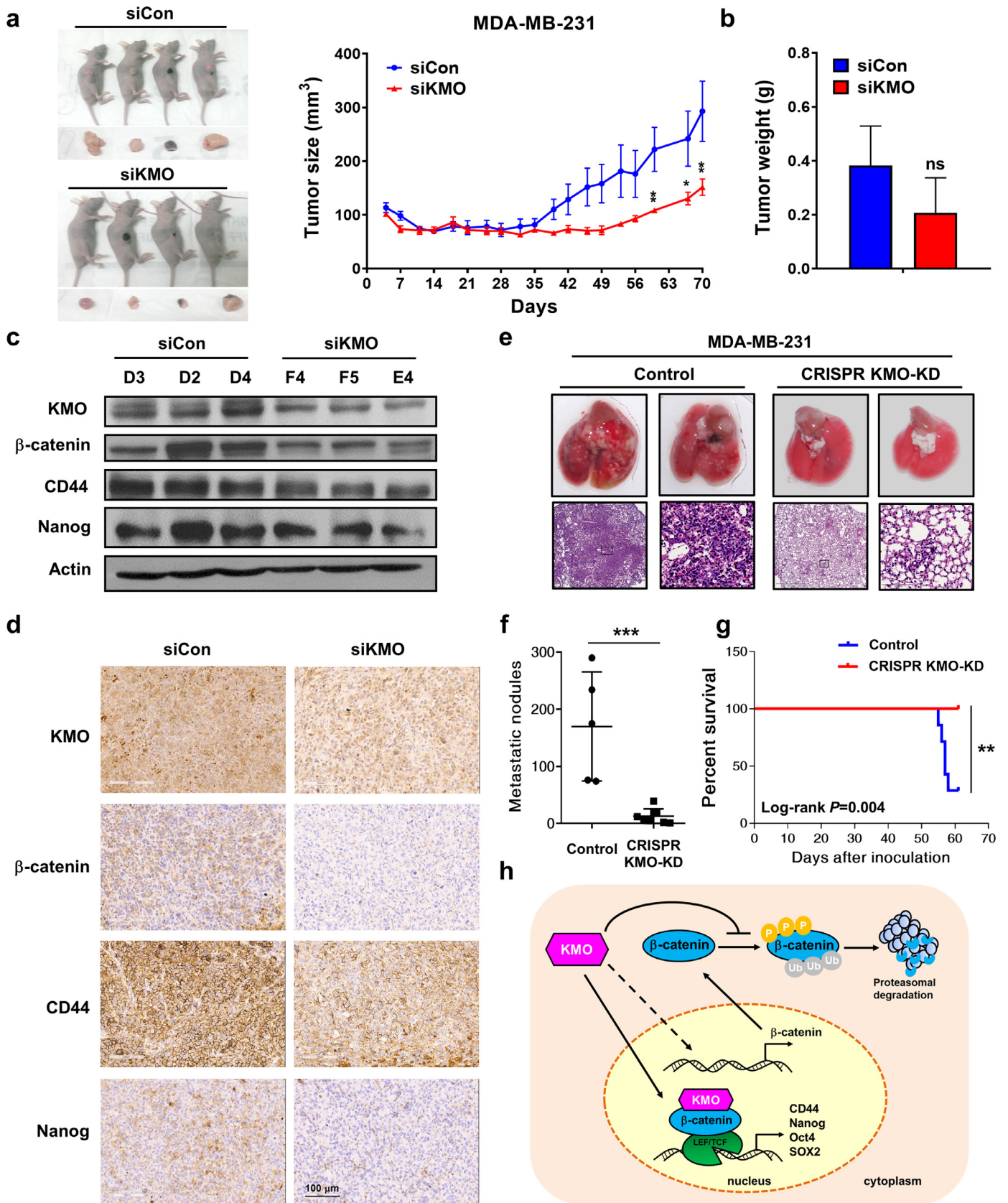


Fig. 6. KMO promotes tumor growth and metastasis of TNBC *in vivo*. (a, b) MDA-MB-231 cells transfected with siRNA against KMO or control for 48 h were subcutaneously injected into nude mice, the xenografted tumors sizes (a) and tumor weights (b) of xenografted mice were measured. (c) The xenografted tumors were analyzed by Western blotting. (d) Immunohistochemical staining of KMO, β -catenin, CD44 and Nanog in xenografted tumors were represented. (e-g) CRISPR KMO-KD and control cells were transplanted into NOD-SCID mice by tail vein injection for H&E staining (e), measurement of metastatic nodules (f) and survival analysis (g). (h) Proposed model for the regulation of KMO/ β -catenin pathway. Points, mean ($N = 4$); columns, mean ($N = 4$); bars, SD. Student's *t*-test, *, $P < 0.05$; **, $P < 0.01$; ***, $P < 0.001$.

exhibits an aberrant metabolic profile [35,36]. For example, TNBC tumors express extremely low levels of members of the miR-200 family, in which miR-200c is a TDO2-targeting repressor, thus permitting TNBC to express TDO2 and genes encoding immunosuppressive factors, such as HMOX-1 and GDF15 [37]. However, the roles of the kynurenine metabolic enzyme KMO in tumors are still ambiguous. Here, we provided evidence that KMO was upregulated in TNBC. Mechanically, KMO elevated β -catenin mRNA expression levels and suppressed β -catenin phosphorylation, thus preventing its degradation. KMO induced pluripotent gene expression through β -catenin, thereby promoting TNBC progression (Fig. 6h).

We observed KMO upregulation in patients with breast cancer and TNBC. Exogenous KMO increased cell proliferation and anchorage-independent growth. In addition, ectopic expression of KMO changed cell morphology from rounded to spindle-shaped and resulted in increased motility and CSC phenotypes. Accumulating evidence indicates that CSCs is a small subpopulation of cancer cells contributing to tumor initiation, growth, metastasis and recurrence [28]. Stemness genes, such as Nanog, OCT4 and SOX2, are responsible for pluripotency maintenance and are also used to identify CSCs [38,39]. Targeting CSCs is a promising therapeutic strategy for cancer, including TNBC [40,41]. However, it should be emphasized that KMO is also overexpressed in other subtypes of breast cancer compared to normal breast tissue. Our findings of the oncogenic role of KMO may not be confined to only TNBC subtype. Comparing to non-TNBC subtypes, where specific pathways, such as HER2 and/or ER signaling, play a major role in each biological subtype, TNBC tends to be more heterogeneous, and several pathways that are not specifically confined to TNBC have emerged as potential therapeutic targets, such as PI3K/Akt and AR pathways. However, given the heterogeneity of TNBC, none of these non-TNBC-specific pathways can be applied as a universal treatment for all TNBC patients; thus, biomarkers are needed [42]. More studies are needed to elucidate the interaction of the KMO/ β -catenin axis and the significance of KMO in the context of HER2-driven breast cancers and/or hormone receptor-positive breast cancer subtypes.

Our results showed that KMO upregulated stemness genes, whereas KMO is a hydroxylase enzyme without a putative DNA-binding element. We found that KMO could be detected in the cytoplasm and nucleus and that knockdown of KMO decreased nuclear β -catenin levels. β -catenin interacts with T-cell factor (TCF) and lymphocyte enhancer transcription factor (LEF) in the nucleus to promote the transcription of multiple genes, leading to abnormal cell progression and growth [16]. In Fig. 4c, we found that knockdown of KMO significantly decreased mRNA level of β -catenin. In addition, we found β -catenin mRNA levels was increased in KMO and KMO mutant overexpressing cells (Fig. 5g). Given the fact that KMO is not a transcriptional factor, we hypothesized that KMO might indirectly altered the transcriptional level of β -catenin by yet-to-be identified mechanisms, or simply this is only a co-incidental finding. Whether KMO could serve as a co-factor in β -catenin transcription also require extensive mechanistic experiments. Based on current data we could not draw any conclusion that KMO upregulates β -catenin in transcriptional level. Interestingly, we demonstrated that KMO interacted with β -catenin and GSK3 β (Fig. 4i, j). Supportive data showed that increased or decreased KMO protein expression levels could affect the amount of phosphorylated β -catenin (Fig. 4f, 4g and S3d). Moreover, using CHX to stop protein synthesis, we demonstrated that KMO significantly delayed the degradation of β -catenin (Fig. 4h). Therefore, it is possible that the protein-protein interactions of KMO with β -catenin and GSK3 β could affect the phosphorylation of β -catenin and, thus, the stability of β -catenin. We observed that the association between GSK3 β and β -catenin and GSK3 β activity was attenuated by KMO expression (Figure S3i). However, the exact molecular mechanisms involved in the binding and phosphorylation remain unknown, and further research is needed. Moreover, despite that we have performed overexpression and knockdown KMO (either

CRISPR or siRNA) to show the association of KMO with β -catenin, further rescue experiments to prove that the effect of altered feature is mainly by KMO are needed, and this is a limitation of current study.

Previous studies have shown that some proteins indirectly enhance β -catenin stability. DACH1 inactivates the Wnt pathway via decreasing p-GSK3 β ^{Ser9} to promote β -catenin degradation [43]. RBMY impairs GSK3 β -dependent β -catenin degradation, inducing stemness properties [44]. CK1 ϵ phosphorylates TCF3, stimulating its binding to β -catenin. TCF3 competes with Axin and APC, preventing β -catenin turnover [45]. We proposed that KMO might modulate β -catenin partly by decreasing p- β -catenin levels. Wnt/ β -catenin signaling is associated with lung and brain metastasis in patients with TNBC [46]. β -catenin has been reported to enhance the migration, stemness and chemosensitivity of TNBC [47]. Moreover, Wnt/ β -catenin pathway blockage inhibits metastasis by reducing breast CSC phenotypes [48]. Our data showed that inhibition of KMO reduced tumor growth and metastasis and that the levels of β -catenin, CD44 and Nanog in tumors were impaired by KMO suppression. In addition, mice inoculated CRISPR KMO-KD cells exhibited longer overall survival than control mice in a metastasis model. It should also be pointed out that the tumor growth of MDA-MB-231 xenografted tumors in nude mice appeared to be suboptimal (Fig. 6a, b). Several technical issues, such as the cytotoxicity of transfection reagents, cell batches, and shear stress during the implantation process might contribute to the relatively slow growth rate of transfected cancer cells.

Several KMO enzymatic inhibitors are being investigated for the treatment of neurodegenerative disease. KMO inhibitors exhibit neuroprotective effects through QA reduction [49]. UPF 648, a 4-aryl-4-oxobutanoic acid derivative, is a KMO substrate analogue and is ineffective at blocking KAT activity. The phenylthiazole benzenesulfonamide Ro 61-8048 is an L-kynurenine analogue with an FAD-binding benzene ring and is a potent and competitive KMO inhibitor [29]. Interestingly, cell viability and migration as well as β -catenin levels were not affected by treatment with the KMO inhibitors UPF 648 and Ro 61-8048. LC-MS data showed that kynurenine levels did not alter but 3-HK level was increased by KMO overexpression. In fact, the levels of kynurenine were much higher than 3-HK in culture medium (data not shown). Our data revealed that the 3-HK to kynurenine ratio was significantly increased suggesting exogenous KMO was enzymatically active. However, KMO harboring N363D or Y398F mutation still upregulated β -catenin and enhanced the cell viability and migration capacity of TNBC cells. These findings suggested that KMO is an oncoprotein and promotes TNBC progression regardless of its enzyme activity.

Kynurenine directly activates aryl hydrocarbon receptor (AhR) to induce regulatory T cell production [50]. TDO2 facilitates kynurenine production, which enhances anchorage-independent survival and metastasis in TNBC by AhR binding and activation [51]. Our findings suggested that the kynurenine metabolic enzyme KMO upregulated β -catenin. Intriguingly, crosstalk between AhR and β -catenin has been reported [52]. AhR activates β -catenin to control breast CSC self-renewal, development and chemoresistance [53]. In inflammatory breast cancer, AhR expression correlates with β -catenin expression, CSCs and poor prognosis [54]. Thus, kynurenine and KMO might enhance TNBC tumorigenesis through an AhR- β -catenin pathway.

Collectively, our study identified KMO as a novel oncoprotein in TNBC. Targeting the KMO/ β -catenin axis might be an attractive approach for TNBC treatment.

Declaration of Competing Interest

The authors declare that they have no competing interests.

Acknowledgements

The laboratory works were completed using facilities from Medical Science & Technology Building of Taipei Veterans General

Hospital. Research was supported by Biobank, Taipei Veterans General Hospital. We thank Dr. Muh-Hwa Yang for providing reporter plasmids Nanog-Luc (Nanog), Oct4-Luc (Oct4), and SOX-2-Luc (SOX-2). We acknowledge the technical services (Affymetrix Expression HU133 2.0) provided by High-throughput Genome and Big Data Analysis Core Facility of the National Yang-Ming University VGH Genome Research Center (VYMG). High-throughput Genome and Big Data Analysis Core Facility is supported by National Core Facility Program for Biotechnology (NCFPB), National Science Council.

Funding Sources

This research was supported by grants from the Taiwan Clinical Oncology Research Foundation; the Yen Tjing Ling Medical Foundation (CI-107-10, CI-108-15); the Ministry of Science and Technology, Taiwan (MOST 104-2628-B-075-001-MY3); Yang-Ming Branch of Taipei City Hospital (10701-62-030; 10801-62-071); Taipei Veterans General Hospital (V106C-101, V107C-025); from Taipei Veterans General Hospital and National Taiwan-University Hospital, and from the Ministry of Health and Welfare, Executive Yuan, Taiwan (MOHW107-TDU-B-212-112015 for the Center of Excellence for Cancer Research at Taipei Veterans General Hospital).

Author contributions

CYL was responsible for coordination and manuscript editing, as well as acting as corresponding authors. TTH, JLC and CHL drafted the manuscript. TTH, CHL, KYL, MFT, YYC, HCL, WLW and TYC conducted *in vitro* and *in vivo* experiments. PYC conducted histopathological experiments. TTH, LMT, JLC and CYL performed or helped with clinical data acquisition and analysis. TTH, LMT, CHL, PYC, JLC, CTH, WLW, HCL, KYL, YFU, MSD and CYL helped with data interpretation and statistical analysis. All the authors had substantial contributions to the conception or design of the work. All the authors read the final manuscript. All the authors agreed with the accuracy and integrity of all parts of the work.

Supplementary materials

Supplementary material associated with this article can be found, in the online version, at doi:10.1016/j.ebiom.2020.102717.

References

- Carey L, Winer E, Viale G, Cameron D, Gianni L. Triple-negative breast cancer: disease entity or title of convenience? *Nat Rev Clin Oncol* 2010;7(12):683–92.
- Pareja F, Geyer FC, Marchio C, Burke KA, Weigelt B, Reis-Filho JS. Triple-negative breast cancer: the importance of molecular and histologic subtyping, and recognition of low-grade variants. *NPJ Breast Cancer* 2016;2:16036.
- Bianchini G, Balko JM, Mayer IA, Sanders ME, Gianni L. Triple-negative breast cancer: challenges and opportunities of a heterogeneous disease. *Nat Rev Clin Oncol* 2016;13(11):674–90.
- Crozier-Reabe KR, Phillips RS, Moran GR. Kynurenine 3-monooxygenase from *Pseudomonas fluorescens*: substrate-like inhibitors both stimulate flavin reduction and stabilize the flavin-peroxy intermediate yet result in the production of hydrogen peroxide. *Biochemistry* 2008;47(47):12420–33.
- Mole DJ, Webster SP, Uings I, et al. Kynurenine-3-monooxygenase inhibition prevents multiple organ failure in rodent models of acute pancreatitis. *Nat Med* 2016;22(2):202–9.
- Zadori D, Veres G, Szalardy L, et al. Inhibitors of the kynurenine pathway as neurotherapeutics: a patent review (2012–2015). *Expert Opin Ther Pat* 2016;26(7):815–32.
- Platten M, Wick W, Van den Eynde BJ. Tryptophan catabolism in cancer: beyond IDO and tryptophan depletion. *Cancer Res* 2012;72(21):5435–40.
- Opitz CA, Litztenburger UM, Sahn F, et al. An endogenous tumour-promoting ligand of the human aryl hydrocarbon receptor. *Nature* 2011;478(7368):197–203.
- Jin H, Zhang Y, You H, et al. Prognostic significance of kynurenine 3-monooxygenase and effects on proliferation, migration, and invasion of human hepatocellular carcinoma. *Sci Rep* 2015;5:10466.
- Chiang Y-L, Lei H-L, Liao AT-C, Chu R-M, Lin C-S. Abstract 4511A: KMO as a novel diagnostic and prognostic biomarker in canine mammary gland tumors. *Cancer Res* 2012;72(8 Supplement):4511A. –4511A.
- Heng B, Lim CK, Lovejoy DB, Bessede A, Gluch L, Guillemin GJ. Understanding the role of the kynurenine pathway in human breast cancer immunobiology. *Oncotarget* 2016;7(6):6506–20.
- Kanaan YM, Sampey BP, Beyene D, et al. Metabolic profile of triple-negative breast cancer in African-American women reveals potential biomarkers of aggressive disease. *Cancer Genom Proteom* 2014;11(6):279–94.
- Clevers H. Wnt/beta-catenin signaling in development and disease. *Cell* 2006;127(3):469–80.
- Orford K, Crockett C, Jensen JP, Weissman AM, Byers SW. Serine phosphorylation-regulated ubiquitination and degradation of beta-catenin. *J Biol Chem* 1997;272(40):24735–8.
- Liu C, Li Y, Semenov M, et al. Control of beta-catenin phosphorylation/degradation by a dual-kinase mechanism. *Cell* 2002;108(6):837–47.
- Krishnamurthy N, Kurzrock R. Targeting the Wnt/beta-catenin pathway in cancer: update on effectors and inhibitors. *Cancer Treat Rev* 2018;62:50–60.
- Bekaii-Saab T, Phelps MA, Li X, et al. Multi-institutional phase II study of selumetinib in patients with metastatic biliary cancers. *J Clin Oncol* 2011;29(17):2357–63.
- Chang CC, Hsu WH, Wang CC, et al. Connective tissue growth factor activates pluripotency genes and mesenchymal-epithelial transition in head and neck cancer cells. *Cancer Res* 2013;73(13):4147–57.
- Liu CY, Huang TT, Chen YT, et al. Targeting SET to restore PP2A activity disrupts an oncogenic CIP2A-feedforward loop and impairs triple negative breast cancer progression. *EBioMedicine* 2019.
- Liu CY, Chu PY, Huang CT, et al. Vartitininib downregulates HER/ERK signaling and induces apoptosis in triple negative breast cancer cells. *Cancers (Basel)* 2019;11(1).
- Fuertig R, Ceci A, Camus SM, Bezdard E, Luippold AH, Hengerer B. LC-MS/MS-based quantification of kynurenine metabolites, tryptophan, monoamines and neopterin in plasma, cerebrospinal fluid and brain. *Bioanalysis* 2016;8(18):1903–17.
- Huang YH, Chu PY, Chen JL, et al. SET overexpression is associated with worse recurrence-free survival in patients with primary breast cancer receiving adjuvant tamoxifen treatment. *J Clin Med* 2018;7(9).
- Nagy A, Lanczky A, Menyhart O, Gyorffy B. Validation of miRNA prognostic power in hepatocellular carcinoma using expression data of independent datasets. *Sci Rep* 2018;8(1):9227.
- Aguirre-Gamboa R, Gomez-Rueda H, Martinez-Ledesma E, et al. SurvExpress: an online biomarker validation tool and database for cancer gene expression data using survival analysis. *PLoS ONE* 2013;8(9):e74250.
- Vaz AP, Ponnusamy MP, Seshacharyulu P, Batra SK. A concise review on the current understanding of pancreatic cancer stem cells. *J Cancer Stem Cell Res* 2014;2.
- Holland JD, Klaus A, Garratt AN, Birchmeier W. Wnt signaling in stem and cancer stem cells. *Curr Opin Cell Biol* 2013;25(2):254–64.
- Malanchi I, Santamaria-Martinez A, Susanto E, et al. Interactions between cancer stem cells and their niche govern metastatic colonization. *Nature*. 2011;481(7379):85–9.
- van der Horst G, Bos L, van der Pluijm G. Epithelial plasticity, cancer stem cells, and the tumor-supportive stroma in bladder carcinoma. *Mol Cancer Res* 2012;10(8):995–1009.
- Smith JR, Jamie JF, Guillemin GJ. Kynurenine-3-monooxygenase: a review of structure, mechanism, and inhibitors. *Drug Discov Today* 2016;21(2):315–24.
- Gao J, Yao L, Xia T, Liao X, Zhu D, Xiang Y. Biochemistry and structural studies of kynurenine 3-monooxygenase reveal allosteric inhibition by RO 61-8048. *FASEB J* 2018;32(4):2036–45.
- Lee A, Djamgoz MBA. Triple negative breast cancer: emerging therapeutic modalities and novel combination therapies. *Cancer Treat Rev* 2018;62:110–22.
- Tang X, Lin CC, Spasojevic I, Iversen ES, Chi JT, Marks JR. A joint analysis of metabolomics and genetics of breast cancer. *Breast Cancer Res* 2014;16(4):415.
- Dewi DL, Mohapatra SR, Blanco Cabanes S, et al. Suppression of indoleamine-2,3-dioxygenase 1 expression by promoter hypermethylation in ER-positive breast cancer. *Oncotarget* 2017;6(2):e1274477.
- Noonepalle SK, Gu F, Lee EJ, et al. Promoter methylation modulates indoleamine 2,3-Dioxygenase 1 induction by activated t cells in human breast cancers. *Cancer Immunol Res*. 2017;5(4):330–44.
- Pelicano H, Zhang W, Liu J, et al. Mitochondrial dysfunction in some triple-negative breast cancer cell lines: role of mTOR pathway and therapeutic potential. *Breast Cancer Res* 2014;16(5):434.
- Lanning NJ, Castle JP, Singh SJ, et al. Metabolic profiling of triple-negative breast cancer cells reveals metabolic vulnerabilities. *Cancer Metab* 2017;5:6.
- Rogers TJ, Christenson JL, Greene LI, et al. Reversal of triple-negative breast cancer EMT by miR-200c decreases tryptophan catabolism and a program of immunosuppression. *Mol Cancer Res* 2019;17(1):30–41.
- Papaccio F, Paino F, Regad T, Papaccio G, Desiderio V, Tirino V. Concise review: cancer cells, cancer stem cells, and mesenchymal stem cells: influence in cancer development. *Stem Cells Transl Med* 2017;6(12):2115–25.
- Liu A, Yu X, Liu S. Pluripotency transcription factors and cancer stem cells: small genes make a big difference. *Chin J Cancer* 2013;32(9):483–7.
- Cazet AS, Hui MN, Elsworth BL, et al. Targeting stromal remodeling and cancer stem cell plasticity overcomes chemoresistance in triple negative breast cancer. *Nat Commun* 2018;9(1):2897.
- Nassar D, Blanpain C. Cancer stem cells: basic concepts and therapeutic implications. *Annu Rev Pathol* 2016;11:47–76.

- [42] Garrido-Castro AC, Lin NU, Polyak K. Insights into molecular classifications of triple-negative breast cancer: improving patient selection for treatment. *Cancer Discov* 2019;9(2):176–98.
- [43] Liu Y, Zhou R, Yuan X, et al. DACH1 is a novel predictive and prognostic biomarker in hepatocellular carcinoma as a negative regulator of Wnt/beta-catenin signaling. *Oncotarget* 2015;6(11):8621–34.
- [44] Chua HH, Tsuei DJ, Lee PH, et al. RBMY, a novel inhibitor of glycogen synthase kinase 3beta, increases tumor stemness and predicts poor prognosis of hepatocellular carcinoma. *Hepatology* 2015;62(5):1480–96.
- [45] Lee E, Salic A, Kirschner MW. Physiological regulation of [beta]-catenin stability by Tcf3 and CK1epsilon. *J Cell Biol* 2001;154(5):983–93.
- [46] Dey N, Barwick BG, Moreno CS, et al. Wnt signaling in triple negative breast cancer is associated with metastasis. *BMC Cancer* 2013;13:537.
- [47] Xu J, Prosperi JR, Choudhury N, Olopade OI, Goss KH. beta-Catenin is required for the tumorigenic behavior of triple-negative breast cancer cells. *PLoS ONE* 2015;10(2):e0117097.
- [48] Jang GB, Kim JY, Cho SD, et al. Blockade of Wnt/beta-catenin signaling suppresses breast cancer metastasis by inhibiting CSC-like phenotype. *Sci Rep* 2015;5:12465.
- [49] Carpenedo R, Meli E, Peruginelli F, Pellegrini-Giampietro DE, Moroni F. Kynurenine 3-mono-oxygenase inhibitors attenuate post-ischemic neuronal death in organotypic hippocampal slice cultures. *J Neurochem* 2002;82(6):1465–71.
- [50] Mezrich JD, Fechner JH, Zhang X, Johnson BP, Burlingham WJ, Bradfield CA. An interaction between kynurenine and the aryl hydrocarbon receptor can generate regulatory T cells. *J Immunol* 2010;185(6):3190–8.
- [51] D'Amato NC, Rogers TJ, Gordon MA, et al. A TDO2-AhR signaling axis facilitates anoikis resistance and metastasis in triple-negative breast cancer. *Cancer Res* 2015;75(21):4651–64.
- [52] Schneider AJ, Branam AM, Peterson RE. Intersection of AHR and Wnt signaling in development, health, and disease. *Int J Mol Sci* 2014;15(10):17852–85.
- [53] Al-Dhfyhan A, Alhoshani A, Korashy HM. Aryl hydrocarbon receptor/cytochrome P450 1A1 pathway mediates breast cancer stem cells expansion through PTEN inhibition and beta-Catenin and Akt activation. *Mol Cancer* 2017;16(1):14.
- [54] Mohamed HT, Gadalla R, El-Husseiny N, et al. Inflammatory breast cancer: activation of the aryl hydrocarbon receptor and its target CYP1B1 correlates closely with Wnt5a/beta-catenin signalling, the stem cell phenotype and disease progression. *J Adv Res* 2019;16:75–86.